

Elsevier required licence: © <2018>. This manuscript version is made available under the CC-BY-NC-ND 4.0 license <http://creativecommons.org/licenses/by-nc-nd/4.0/>

1 **Ferrous ion as reducing agent in the generation of antibiofilm nitric oxide**
2 **from copper-based catalytic system**

3 *Vita Wonoputri^{1,2}, Cindy Gunawan^{1,3,*}, Sanly Liu¹, Nicolas Barraud⁴, Lachlan H. Yee^{5,*}, May*
4 *Lim¹, Rose Amal¹*

5

6 ¹Particles and Catalysis Research Group, School of Chemical Engineering, The University of New
7 South Wales, Sydney, NSW 2032, Australia

8 ²Department of Chemical Engineering, Institut Teknologi Bandung, Bandung 40132, Indonesia

9 ³ithree institute, University of Technology Sydney, NSW 2007, Australia

10 ⁴Genetics of Biofilms Unit, Department of Microbiology, Institut Pasteur, 75015 Paris, France

11 ⁵Marine Ecology Research Centre in the School of Environment, Science and Engineering,
12 Southern Cross University, Lismore, NSW 2480, Australia

13 E-mail: Cindy.Gunawan@uts.edu.au; lachlan.yee@scu.edu.au

14

15 Keywords: biofilm, antibiofilm, nitric oxide, copper, catalyst, iron

16

17 The work found that the electron-donating properties of ferrous ions (Fe^{2+}) can be used for the
18 conversion of nitrite (NO_2^-) into the biofilm-dispersing signal nitric oxide (NO) by a copper(II)
19 complex (CuDTTCT) catalyst, a potentially applicable biofilm control technology for the water
20 industries. The availability of Fe^{2+} varied depending on the characteristics of the aqueous systems
21 (phosphate- and carbonate-containing nitrifying bacteria growth medium, NBGM and phosphate
22 buffered saline, PBS at pH 6 to 8, to simulate conditions typically present in the water industries)
23 and was found to affect the production of NO from nitrite by CuDTTCT (casted into PVC). Greater
24 amounts of NO were generated from the CuDTTCT-nitrite- Fe^{2+} systems in PBS compared to those
25 in NBGM, which was associated with the reduced extent of Fe^{2+} -to- Fe^{3+} autoxidation by the iron-

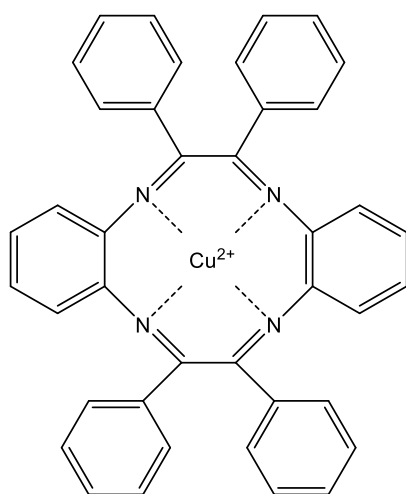
26 precipitating moieties phosphates and carbonate in the former system. Further, acidic conditions
27 at pH 6.0 were found to favor NO production from the catalytic system in both PBS and NBGM
28 compared to neutral or basic pH (pH 7.0 or 8.0). Lower pH was shown to stabilize Fe^{2+} and reduce
29 its autoxidation to Fe^{3+} . These findings will be beneficial for the potential implementation of the
30 NO-generating catalytic technology and indeed, a ‘non-killing’ biofilm dispersal activity of
31 CuDTTCT-nitrite- Fe^{2+} was observed on nitrifying bacteria biofilms in PBS at pH 6.

32 **1. Introduction**

33 Biofilms are microbial communities that grow within a matrix of extracellular polymeric
34 substances, and are known to cause problems in water industries. In many cases, biofilm formation
35 can decrease heat exchanger or cooling tower efficiency [1]. Biofilm growth in water distribution
36 pipelines could also lead to microbial induced corrosion [2]. Moreover, biofilms have been found
37 to act as a reservoir for the spread of antibiotic resistance genes [3,4]. Conventional methods to
38 control microbial growth using disinfectants such as chlorine and chloramine, are often ineffective
39 at eradicating biofilms due to their increased resistance compared to the free-floating (planktonic)
40 biomass [5]. Therefore, an alternative method for biofilm eradication is required. The utilization
41 of nitric oxide (NO) with its proven efficacy in controlling biofilm formation, appears to be an
42 attractive solution. NO is a free radical gas capable of dispersing biofilms, reverting the biomass
43 to planktonic state via a non-toxic pathway [6,7]. Due to its high reactivity and short half-life,
44 research efforts have been dedicated toward the development of sustainable NO generation
45 technologies, capable of delivering NO to the target site [8].

46 Our previous work has reported the use of a copper(II) complex (copper(II) dibenzo[e,k]-
47 2,3,8,9-tetraphenyl-1,4,7,10-tetraaza-cyclododeca-1,3,7,9-tetraene or CuDTTCT, **Scheme 1**) that
48 is embedded in a poly(vinyl chloride) (PVC) matrix, to function as a NO generating catalyst [9,10].

49 The utilization of this copper(II) complex with ascorbic acid as reducing agent generates an active
50 copper(I) species that converts nitrite (typically present in water) to NO [9–12]. The NO-
51 generating catalytic system was able to suppress the growth of nitrifying bacteria, a biofilm-
52 forming consortium commonly found in chloraminated water, as well as dispersing pre-formed
53 nitrifying biofilms [9]. Indeed, our work has also shown the capability of the catalytic system to
54 likely utilize endogenous nitrite (produced by nitrifying bacteria biofilms) for NO production [10].
55 Yet, the necessity of using an exogenous reducing agent such as ascorbate may not be favorable
56 for various applications of this catalytic system in the water industry. In contrast, the possibility of
57 exploiting naturally present chemical moieties (in water) capable of reducing the copper(II)
58 complex catalyst offers a promising alternative. Potential candidates are for instance, humic
59 substances, which have been shown to reduce copper(II) to copper(I) under natural water
60 conditions [13]. Such presence of organic matters however, is generally unwanted in
61 chlorinated/chloraminated water systems due to the likely formation of disinfection by-products.
62 Another inorganic moiety commonly occurring in water systems that holds great potential as a
63 reducing agent is the ferrous ion (Fe^{2+}) [14,15].



64 **Scheme 1.** CuDTTCT Structure
65

66 Iron usually undergoes chemical (and photochemical) reactions resulting in its rapid cycling
67 between ferrous (Fe^{2+}) and ferric (Fe^{3+}) forms [14,15]. Fe^{2+} ions have been reported to reduce
68 copper(II) species to copper(I) and such interactions could occur either homogeneously (both
69 copper and iron species in solution) or heterogeneously (only copper or iron species in solution)
70 [16]. For instance, oxidation of Fe^{2+} ions in seawater conditions is enhanced by 0.4 log units in the
71 presence of Cu^{2+} ion and, in turn, a strong and rapid reduction of Cu^{2+} to Cu^+ was observed [17].
72 In other cases, solid iron in the form of green rusts – a mixed iron(II)/iron(III) hydroxides, have
73 been found to rapidly reduce aqueous Cu^{2+} ion to form solid metallic copper [18]. Contact killing
74 of bacteria on solid iron surface was also observed when it is used in conjunction with Cu^{2+} , which
75 was attributed to the reduction of Cu^{2+} to form the toxic Cu^+ by the iron surface [19]. In this study,
76 the use of Fe^{2+} (in the form of ferrous chloride) as an alternative reducing agent for the CuDTTCT
77 catalyst (casted into PVC) was investigated in aqueous systems of different characteristics, which
78 contain moieties typically found in the water industries. The pH 6 to 8 aqueous systems contain
79 the iron-precipitating moieties phosphates and carbonate (normally present in water) [20-22] that
80 will affect the Fe^{2+} availability and in turn, the NO-producing capabilities of the catalyst.
81 Ultimately, the effectiveness of the catalytic system in dispersing pre-formed nitrifying bacteria
82 biofilms was investigated.

83 **2. Material and methods**

84 *Synthesis of dibenzo[e,k]-2,3,8,9-tetraphenyl-1,4,7,10-tetraaza-cyclododeca-1,3,7,9-tetraene*
85 *complex (DTTCT) and its copper complex*

86 The syntheses of dibenzo[e,k]-2,3,8,9-tetraphenyl-1,4,7,10-tetraaza-cyclododeca-1,3,7,9-
87 tetraene (DTTCT), its copper complex, and the coupon samples were performed following the
88 method described elsewhere [9]. In brief, benzil (0.05 mol; Aldrich 98%) and o-phenylenediamine

89 (0.05 mol; Aldrich, 99.5%) were refluxed in ethanol with few drops of hydrochloric acid (Ajax
90 Finechem, 32%) for 6 hours at 80 °C. The resultant DTTCT (0.01 mol) was mixed with copper
91 acetate monohydrate (0.05 mol; Ajax APS) in ethanol and refluxed at 80 °C for 6 hours.

92 The coupons were synthesized by mixing the copper complex (2 mg) with pre-dissolved PVC
93 (Chemson Pacific Pty Ltd) in tetrahydrofuran (THF, Chem-Supply) solution (0.3 mL, 66 mg/L) in
94 an ultrasonic bath. Round glass cover slips (18 mm diameter, ProSciTech) were washed with dilute
95 nitric acid, acetone, and ethanol followed by overnight drying at 110 °C before being used as the
96 cast template. Bare coupon (PVC without any copper complex, typical weight ~20 mg) was used
97 as the control. The coupons were dried at 50 °C for 12 hours and peeled off from the glass cover
98 slips. Characterizations of the ligand, complex, and coupons have been presented elsewhere [9].

99 *NO generation measurement*

100 NO generation from the catalytic system was measured amperometrically using an Apollo
101 TBR4100 Free Radical Analyzer (World Precision Instrument) equipped with ISO-NOP 2 mm
102 probe. The system was calibrated using *S*-nitroso-*N*-acetylpenicillamine (SNAP; Sigma) and
103 copper sulfate solution according to manufacturer's protocol. CuDTTCT coupons or bare coupons
104 were placed at the bottom of a 20 mL glass vials equipped with stir bars and filled with 10 mL of
105 testing solution, either the nitrifying bacteria growth medium, the 'NBGM' (ATCC medium 2265
106 with final pH of 8.0, consisting of three different stock solutions – stock 1 (final composition in
107 the medium mixture): 25 mM (NH₄)₂SO₄, 3 mM KH₂PO₄, 0.7 mM MgSO₄, 0.2 mM CaCl₂, 0.01
108 mM FeSO₄, 0.02 mM EDTA, 0.5 μM CuSO₄; stock 2: 40 mM KH₂PO₄, 4 mM NaH₂PO₄, adjusted
109 to pH 8 by 10 M NaOH; stock 3: 4 mM Na₂CO₃) or PBS (consists of 137 mM NaCl, 2.7 mM KCl,
110 10 mM Na₂HPO₄ and 1.8 mM KH₂PO₄, prepared using PBS tablet from Sigma). **NBGM** at pH 6

111 was prepared by adjusting pH of stock 2 from 4.5 to 5.5 by 10 M NaOH, and mixing it with stock
112 1 and 3. Concentrated hydrochloric acid was used to adjust the pH of phosphate buffer from 7.4 to
113 7.0, 6.5, and 6.0. Measurement of the pH was performed using a pH Lab Meter (Metrohm 827,
114 measuring resolution of 0.001 pH) and the pH meter was calibrated before each use. Bare or
115 CuDTTCT coupon was placed at the bottom of the vial and measurement probe was placed
116 approximately 1 cm from the coupon. Sodium nitrite (Ajax Finechem) and iron(II) chloride
117 tetrahydrate (Sigma Aldrich, $\geq 99\%$) was used as the catalytic reactant. At the end of the
118 measurement, an NO scavenger namely 2-Phenyl-4,4,5,5-tetramethylimidazoline-1-oxyl 3-oxide
119 (PTIO; Alexis Biochemicals) was added to re-establish the baseline. All measurements were
120 performed in the presence of ambient oxygen.

121 *Iron speciation analysis*

122 The concentration of $\text{Fe}^{2+}/\text{Fe}^{3+}$ in the solution was analyzed over time *via* ferrozine
123 spectroscopy method. Colour reagent ferrozine (Aldrich), reducing agent hydroxylamine
124 hydrochloric acid (Sigma Aldrich), and ammonium acetate buffer (Ajax) were prepared as
125 described by Viollier etc [20]. Two mL of sample solution was added into 12 well plates (Corning)
126 containing either PVC coupon or CuDTTCT coupon, followed by addition of equimolar amount
127 of nitrite and Fe^{2+} . Iron speciation measurement was performed for two hours, with two 100 μL
128 aliquots of the sample were collected every 3 minutes or 20 minutes. The first aliquots were treated
129 with ferrozine and represent the concentration of Fe^{2+} while the second aliquots were treated with
130 ferrozine, reducing agent and buffer to depict the concentration of total iron. The absorbance of
131 the Fe^{2+} -ferrozine complex after incubation of 5 min in room temperature was measured using
132 UV-Vis spectrophotometer (Varian Cary 300) at 562 nm.

133

134 *Biofilm assay*

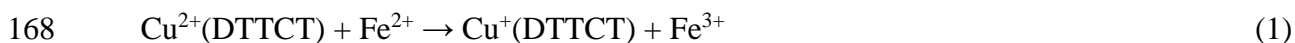
135 Biofilm was formed from a commercial mixed inoculum of nitrifying bacteria (Aquasonic Bio-
136 Culture) which consists of *Nitrosospira multiformis*, *Nitrosospira marina*, and *Bacillus* sp.
137 (Aquasonic Bio-Culture). One milliliter of the mixed inoculum was added into 100 mL of the
138 NBGM and incubated for 3 days in the dark (30 °C, 100 rpm). The three-day-old culture was then
139 inoculated into fresh NBGM medium at 1 : 100 ratio and 2 mL aliquots (OD = 0.008) were added
140 into 35 mm culture dishes with a coverglass bottom (internal glass diameter 22 mm, ProSciTech)
141 with the presence of the bare (PVC-only) or CuDTTCT (embedded in PVC) coupon. In these
142 systems, the biofilm was grown for 3 days in the dark (30 °C, 100 rpm). Note that the amount of
143 copper ion leaching from the CuDTTCT was minimal (< 1%), detected during the 3-day incubation
144 period) [9]. For the biofilm dispersal assay, one hour before incubation ended, the supernatants
145 were removed and centrifuged at 10,000 rpm for 15 mins to isolate the planktonic bacteria.
146 Meanwhile, PBS pH 7.4 was added to the biofilm to prevent the cells from drying. The planktonic
147 bacteria were re-dispersed in sterile PBS pH 6 solution followed by the addition of sodium nitrite
148 and iron(II) chloride to trigger the production of NO, then added back to the respective wells and
149 incubation was continued for one hour. For the biofilm surface coverage analysis, at the end of the
150 second incubation step, planktonic bacteria were removed. The dishes that contain the biofilm
151 were washed twice with PBS to remove the loosely attached cells. The attached cells were stained
152 with 400 µL of staining solution consists of 3.34 µM of SYTO-9 and 19.97 µM of propidium
153 iodide in PBS (LIVE/DEAD® *BacLight*TM Bacterial Viability Kits L-7007, Molecular Probes Inc.)
154 for a minimum of 15 min at room temperature. The attached stained cells were then assessed by
155 confocal laser scanning microscopy (Olympus FluoViewTM FV1000). Twelve images across the
156 glass bottom were acquired and the surface coverage of the biofilm was analyzed using image

157 analysis software (Fiji/ImageJ). Statistical analysis was performed using one-way ANOVA
158 followed by Dunnett post hoc analysis on Prism (GraphPad).

159 **3. Results and Discussion**

160 **3.1. Catalytic NO generation from CuDTTCT-nitrite-Fe²⁺ in different aqueous systems** 161 **and pHs and the effect of Fe²⁺ availability**

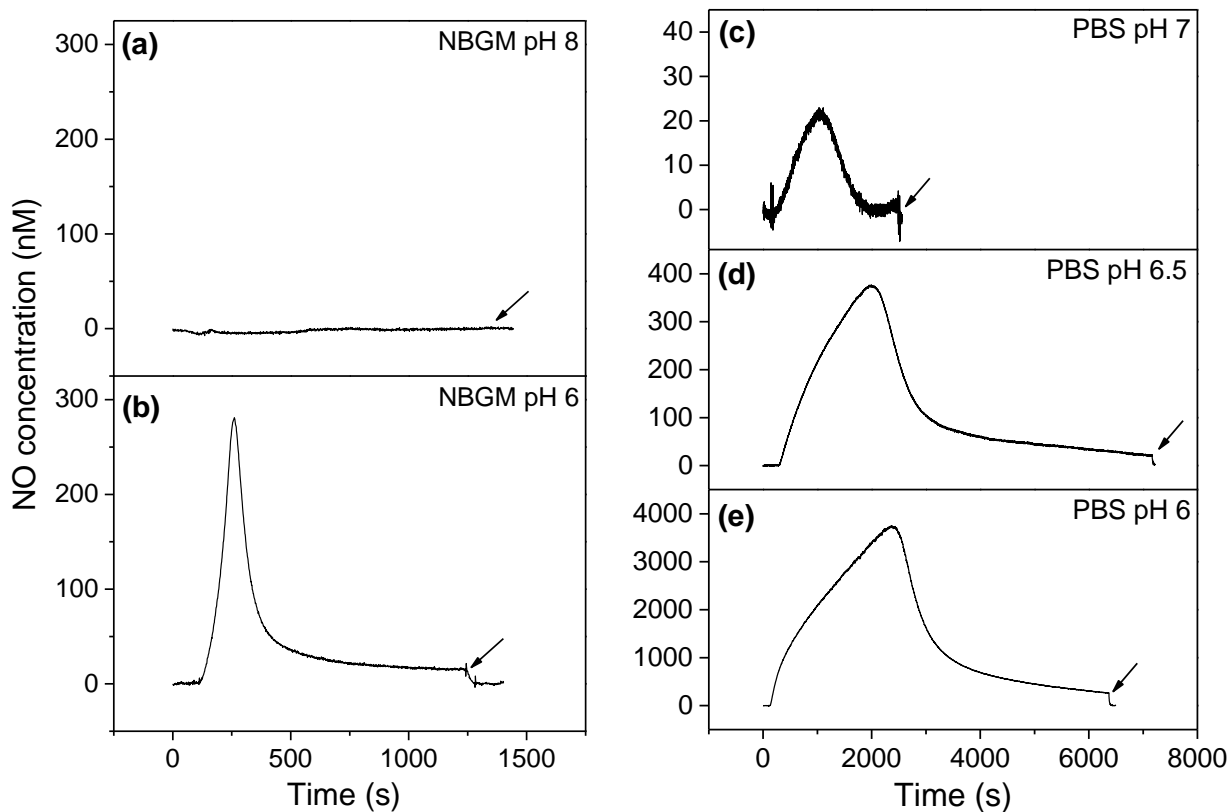
162 To evaluate the capacity of Fe²⁺ as reducing agent for the catalytic conversion of nitrite to NO
163 from CuDTTCT-containing films, we studied the impact of Fe²⁺ on the production of NO under
164 various conditions of aqueous media that are relevant to the water industries – the phosphates- and
165 carbonate-containing and pH-adjustable nitrifying bacteria growth medium (NBGM) and
166 phosphate buffered saline (PBS). The catalytic conversion of nitrite to NO is proposed to occur
167 *via* the redox cycling of copper [9,11,12]:



170 In these experiments, the generation of NO in aqueous media was measured amperometrically (see
171 Experimental section) which allows for instantaneous detection of NO present in solution.

172 First, the CuDTTCT film-nitrite-Fe²⁺ system (0.5 mM equimolar nitrite-Fe²⁺) was tested in
173 NBGM which were adjusted to different pHs. In NBGM at pH 8.0, Fe²⁺ addition to CuDTTCT in
174 the presence of nitrite did not result in any detectable generation of NO (**Figure 1a**). In contrast,
175 at pH 6.0, NO generation was observed, with a peak of 280 nM was observed in the first ~4 min
176 after adding Fe²⁺ (**Figure 1b**). This surge in NO generation was followed by a rapid decrease with
177 only 35 nM instantaneous NO detected at ~8 min and beyond, most likely due to the rapid
178 oxidation of NO with dissolved oxygen (O₂) [9]. An NO scavenger, PTIO was then added into the

179 system, causing an instant drop in the amperometric signal, therefore confirming the NO
180 generation. In these experiments, no change in pH was observed following the addition of nitrite-
181 Fe^{2+} in NBGM (which contains ~65 mM weak acid-base pH-buffering ingredients).



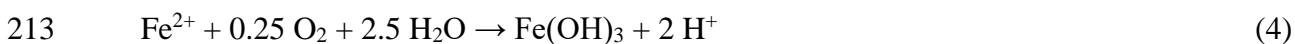
182
183 **Figure 1.** Amperometric measurement of NO generation from CuDTTCT-nitrite- Fe^{2+} system in
184 NBGM at (a) pH 8 and (b) pH 6 or in PBS at (c) pH 7, (d) pH 6.5, and (e) pH 6. 0.5 mM of sodium
185 nitrite was added followed by the addition of 0.5 mM of Fe^{2+} solution. PTIO was added (time of
186 addition was denoted by a black arrow) to re-establish the baseline.
187

188 Next, NO generation from the CuDTTCT-nitrite- Fe^{2+} (0.5 mM equimolar nitrite- Fe^{2+}) system
189 was tested in PBS also adjusted to different pHs. At the pH 7.0, which corresponds to the natural
190 pH of PBS, a maximum 20 nM NO was detected after ~17 min (**Figure 1c**). At pH 6.5, a higher
191 400 nM NO was generated over a longer period of ~33 min (**Figure 1d**). Ultimately, at the lowest
192 pH tested (pH 6), a significantly higher NO concentration of up to 4000 nM was detected after ~42
193 min (**Figure 1e**). In these experiments, only a small pH drop (< 0.1) was observed upon the

194 addition of nitrite-Fe²⁺ in PBS (which contains ~10 mM weak acid-base pH-buffering ingredients).
195 The addition of PTIO further confirms the generation of NO in these catalytic systems and
196 therefore, like those observed in the growth medium, the apparent capability of Fe²⁺ as reducing
197 agent for the redox cycling of copper.

198 Comparing the NO generation behaviour in NBGM and PBS at similar pH (pH 6), ~13-fold
199 higher NO concentration was observed in the latter system and over a longer period. Indeed, NO
200 was still detected even after 100 min of measurement. Previous reports on the catalytic NO
201 production *via* copper redox cycling has demonstrated high dependence on the formation of the
202 active copper(I) species [9,10] and therefore, the adequate presence of Fe²⁺ ions as a reducing
203 agent is vital in determining the NO generation behaviour under different conditions. This
204 observed differences in NO generation, as well as in the NBGM and PBS systems at different pHs,
205 could be attributed to discrepancies in the Fe²⁺ availability in the respective systems, as evident by
206 the iron speciation studies described in the following.

207 Iron speciation analysis was performed following the method by Viollier *et al.* [20], which
208 describes the spectrophotometry measurement of dissolved Fe²⁺/Fe³⁺ concentrations. The iron
209 speciation analysis was first carried out in the absence of CuDTTCT to obtain unambiguous
210 evidence on the potential Fe²⁺-to-Fe³⁺ autoxidation (equation 3) due to the likely interactions of
211 Fe²⁺ with oxygen (equation 3 and 4) and iron-precipitating moieties in NBGM [21].



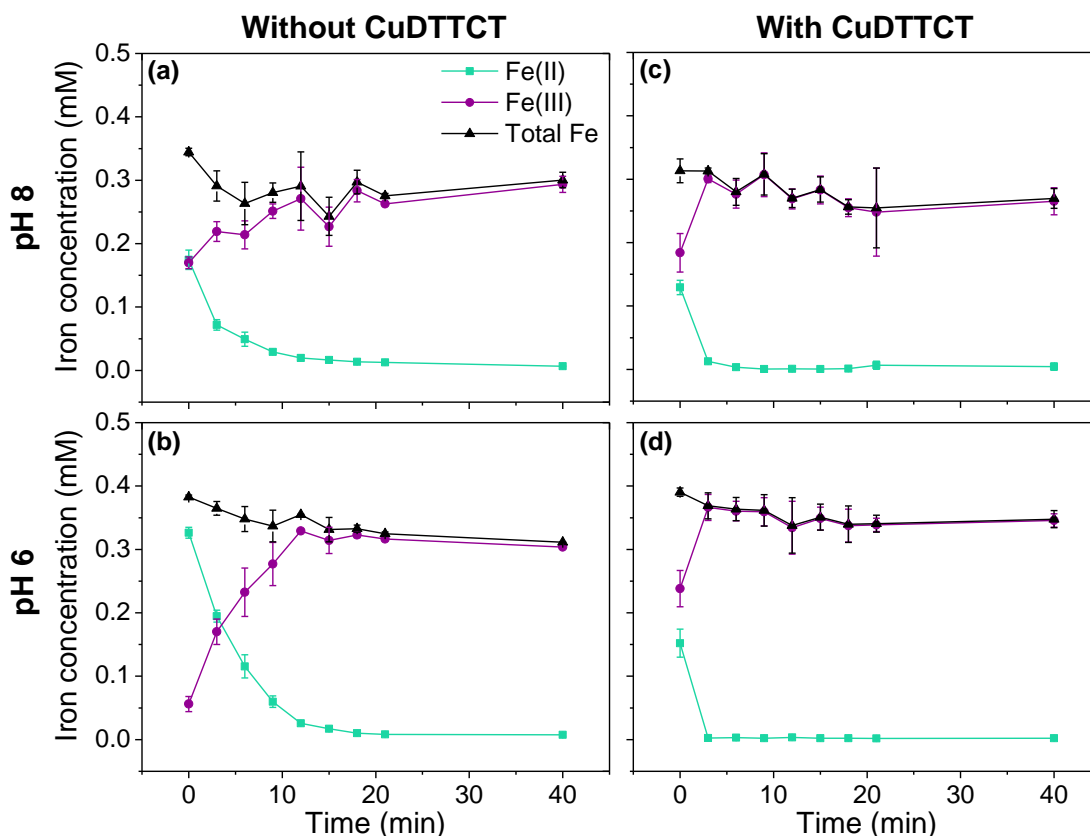
214 In the pH 6 NBGM, the amount of Fe²⁺ available in the absence of copper (bare or PVC-only
215 film) was ~0.33 mM at time 0 (**Figure 2b**), while only ~0.17 mM was present at pH 8 (**Figure 2a**).
216 It should be noted that a 10 s time lag occurs between the addition of Fe²⁺ and the first point of

217 sampling (time 0). The lower initial Fe²⁺ concentration at pH 8 could be attributed to the rapid
 218 autoxidation of Fe²⁺ to Fe³⁺ at higher pH [17,22]. Beyond this initial time, further Fe²⁺-to-Fe³⁺
 219 autoxidation was apparent in both systems; the presence of Fe²⁺ at pH 6 was depleted at 18 min,
 220 while it only took 10 min for depletion of Fe²⁺ at pH 8. The presence of phosphates (~47 mM) in
 221 NBGM is thought to aid the Fe²⁺-to-Fe³⁺ autoxidation reaction. Fe²⁺ could react with phosphate to
 222 form iron-phosphate species, including iron-hydroxyphosphate (equation 5) and iron(III)-
 223 phosphate (equation 6) precipitates [21,23,24]. In the case of iron(III)-phosphate formation, this
 224 reaction is preceded by the oxidation of Fe²⁺ to Fe³⁺ (as written in equation 3)



227 Indeed, a decrease in total soluble iron concentration from 0.5 mM added iron to ~0.3 mM detected
 228 at the end of the experiment in both systems, indicating precipitation of iron out of the solution
 229 (**Figure 2a, b**). The presence of carbonates (4 mM) in NBGM has also been reported to assist in
 230 iron precipitation forming FeCO₃ (equation 7) and Fe(CO₃)₂²⁻ (equation 8) [17,25].





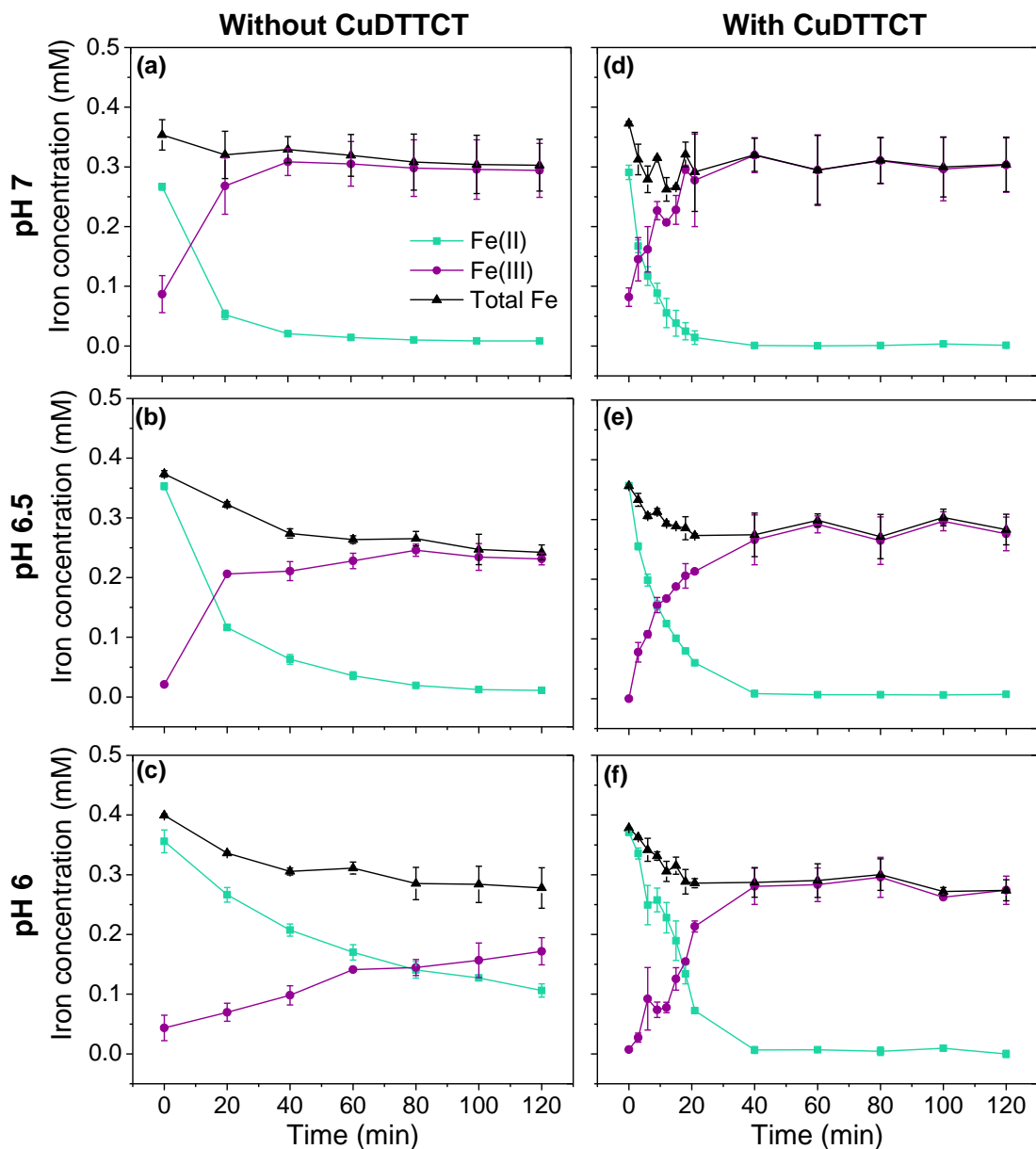
233

234 **Figure 2.** Change in Fe^{2+} oxidation state over time in the presence of bare film and nitrite in NBGM
 235 at (a) pH 8 and (b) pH 6; in the presence of CuDTTCT film and nitrite in NBGM at (c) pH 8 and
 236 (d) pH 6. Theoretical concentrations of nitrite and iron used are 0.5 mM.
 237

238 When CuDTTCT was present in NBGM, the oxidation of Fe^{2+} to Fe^{3+} occurred at a significantly
 239 faster rate, Fe^{2+} was depleted in 3 min at both pH 6 and 8 (**Figure 2c** and d). This is most likely
 240 due to interaction between the Fe^{2+} ions in the solution with the copper complex inside the PVC
 241 matrix, *i.e.* Fe^{2+} as reducing agent, facilitating the copper(II)/copper(I) redox cycling and in turn,
 242 resulting in the observed NO generation in the presence of nitrite (**Figure 1b**). Unlike that of at pH
 243 6 however, the apparent interaction between copper and Fe^{2+} at pH 8 did not result in NO
 244 generation (**Figure 1a**). This is thought to result from the earlier mentioned lower Fe^{2+} initial
 245 availability at pH 8 (~0.17 mM at time 0, **Figure 2a**) compared to that of at pH 6 (~0.33 mM at
 246 time 0, **Figure 2b**) due to Fe^{2+} -to- Fe^{3+} autoxidation. To test for any potential factor other than the

247 Fe^{2+} autoxidation that could account for the absence of NO generation, an excess Fe^{2+} (1 mM) was
248 added to pH 8 NBGM containing soluble Cu^{2+} and in the presence of nitrite (1 mM). Indeed, we
249 detected NO generation and again, none with the added presence of 0.5 mM Fe^{2+} (Supplementary
250 Figure 1). This indicate that Fe^{2+} availability is a major factor in the NO generation.

251 Next, we carried out the iron speciation analysis in PBS, first, in the absence of CuDTTCT
252 (PVC-only/control film). At the highest pH tested (pH 7), Fe^{2+} autoxidation was completed in 40
253 min (**Figure 3a**), while at pH 6.5, Fe^{2+} was depleted after 100 min (**Figure 3b**). Fe^{2+} autoxidation
254 was the slowest at pH 6, with ~ 0.1 mM of iron(II) still detected at 120 min (**Figure 3c**) (also note
255 the lower ~ 0.27 mM initial Fe^{2+} concentration at pH 7 compared to ~ 0.36 mM at pH 6.5 and 6).
256 Recalling the Fe speciation-time profile in NBGM at pH 6 with no CuDTTCT, it is clear that Fe^{2+}
257 autoxidation occurred slower in the PBS compared to in NBGM. Considering the presence of
258 lower concentrations of iron-precipitating agents in the PBS (*e.g.* PBS contains four times lower
259 phosphate than in NBGM), this suggests higher availability of Fe^{2+} ions in the PBS as reducing
260 agent for the catalytic NO generating system, which most likely led to the observed 13-fold higher
261 NO generation in pH 6 PBS (up to 4000 nM) compared to that of in NBGM at pH 6 (up to 280
262 nM). NBGM also contains EDTA (0.02 mM), which could complex with Fe^{2+} , therefore reducing
263 the Fe^{2+} availability even further.



264

265 **Figure 3.** Change in Fe²⁺ oxidation state over time in the presence of bare film and nitrite in PBS
 266 at (a) pH 7, (b) pH 6.5 and (c) pH 6; in the presence of CuDTTCT film and nitrite in PBS at (d)
 267 pH 7, (e) pH 6.5 and (f) pH 6. Theoretical concentrations of nitrite and iron used are 0.5 mM.
 268

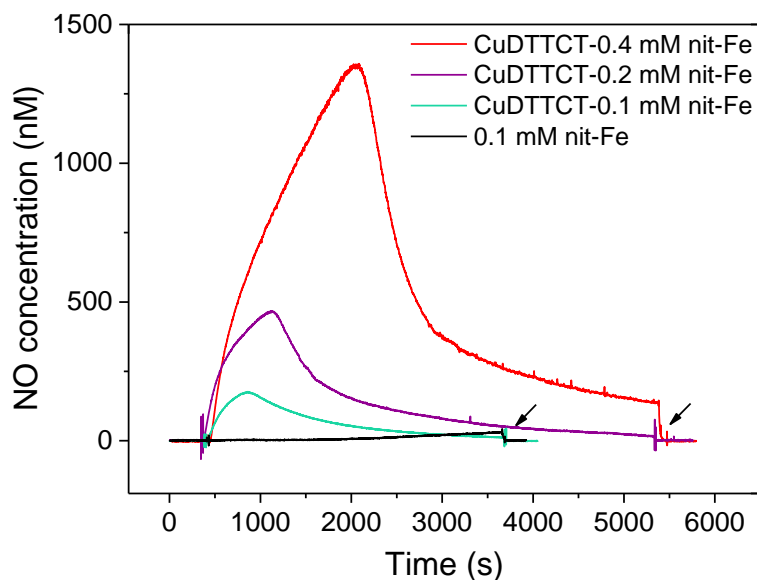
269 Similar to the observation in NBGM, Fe²⁺ oxidation in PBS occurred faster in the presence of
 270 CuDTTCT compared to that in the absence of CuDTTCT (**Figure 3d, e, f**). In the presence of
 271 CuDTTCT, Fe²⁺ oxidation was completed in 20 min at pH 7, while it took 40 min for complete
 272 depletion of Fe²⁺ at pH 6.5 and 6. The observations again indicate the copper-iron interactions,

273 that is, the role of Fe^{2+} as reducing agent in copper(II)/copper(I) redox cycling for the detected
274 generation of NO (**Figure 1c, d, e**) and that such interactions could occur at all tested pH of 6 to
275 7, in agreement with earlier reports [17]. Different pHs however, gave rise to different NO
276 generation profile. The highest NO generation at pH 6 could be attributed to first, the relatively
277 high Fe^{2+} initial availability (~ 0.36 mM at time 0, **Figure 3c**) in comparison to initial Fe^{2+} at pH 7
278 (~ 0.27 mM at time 0, **Figure 3a**) and second, to the slower Fe^{2+} oxidation at pH 6. Further, it has
279 been reported that nitrite will form nitrous acid ($\text{pK}_a \sim 3.3$) at acidic pH and in turn, decompose
280 into NO [26]. Such non-catalytic origin of NO generation, as later described, could also contribute
281 to the increasing NO detection at pH 7, 6.5 and 6 respectively.

282 **3.2. Effect of nitrite and Fe^{2+} concentration on NO generation from CuDTTCT-nitrite-** 283 **Fe^{2+} catalytic systems**

284 The effect of different concentration of nitrite and Fe^{2+} on NO generation was investigated in
285 PBS pH 6 (**Figure 4**). When 0.1 mM equimolar nitrite- Fe^{2+} alone is present in the system (no
286 CuDTTCT), a slow build-up of low concentration of NO was observed, with 30 nM NO detected
287 at 60 min (**Figure 4**, black line), which is thought to result from the earlier mentioned dissociation
288 of nitrous acid to form NO at the acidic pH and/or the known slow decomposition of nitrite in the
289 presence of iron [11,26,27]. The presence of CuDTTCT in comparable system saw generation of
290 up to 200 nM NO from nitrite in the first ~ 15 min, again, most likely resulting from the
291 copper(II)/copper(I) redox cycling facilitated by the presence of Fe^{2+} . Upon increasing the nitrite
292 and Fe^{2+} concentration, an enhanced generation of NO was observed, with detection of up to 1300
293 nM NO in CuDTTCT system with 0.4 mM nitrite- Fe^{2+} concentration. The time required to reach
294 maximum NO generation was longer with the increasing nitrite- Fe^{2+} concentration. For instance,
295 it took ~ 35 min for the CuDTTCT-0.4 mM nitrite- Fe^{2+} system to reach its maximum NO

296 generation and only ~15 min for the CuDTTCT-0.1 mM nitrite-Fe²⁺ system. The NO concentration
297 dropped upon reaching the maximum concentration, which is thought to result from the depletion
298 of Fe²⁺ in the system as previously described (**Figure 3f**). Again, an instant drop in the
299 amperometric signal upon addition of PTIO (black arrow, **Figure 4**) confirmed the NO generation.



300
301 **Figure 4.** Amperometric measurements of NO generation from CuDTTCT-nitrite-Fe²⁺ system.
302 After stable baseline was observed, sodium nitrite was added followed by the addition of equimolar
303 concentration of Fe²⁺ solution. PTIO (black arrow) was added to re-establish the baseline.
304

305 3.3. Biofilm dispersal by the NO-generating CuDTTCT-nitrite-Fe²⁺ systems

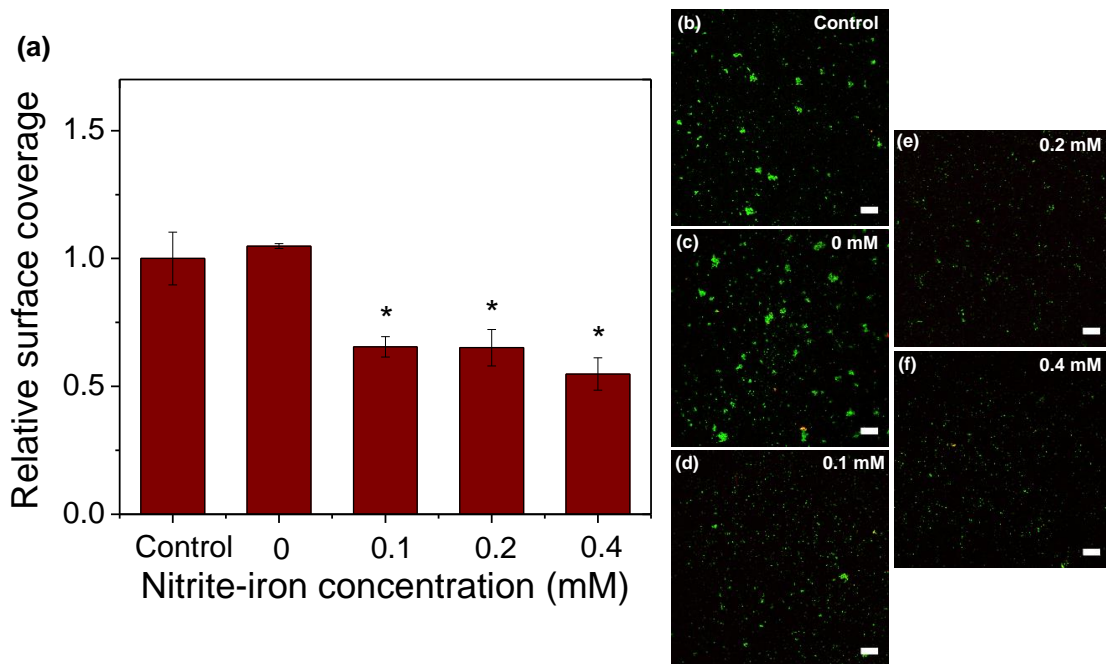
306 The ability of the catalytically generated NO from the CuDTTCT-nitrite-Fe²⁺ systems to
307 disperse pre-formed nitrifying bacteria biofilm was investigated. The model biofilm was grown
308 for 3 days from a mixed inoculum of nitrifying bacteria in growth medium and further biofilm
309 dispersal study was carried out in PBS pH 6 to simulate the pH drop in water utilities with heavy
310 growth of nitrifying biofilms due to nitrification [28]. At maturation, the formed nitrifying biofilm
311 was re-suspended in PBS pH 6 following removal of the growth medium. Re-suspension of the
312 biofilm in PBS pH 6 did not cause any premature biofilm dispersal, as evident by the comparable

313 biofilm surface coverage as that of prior to the removal of the growth medium (Supplementary
314 Figure 2), in agreement with previous report [29].

315 The treatment of the pre-formed biofilm in CuDTTCT system with presence of 0.1 mM and 0.2
316 mM equimolar nitrite-Fe²⁺ resulted in ~35% reduction in biofilm surface coverage after 1 h
317 (analysed by confocal laser scanning microscopy) compared to the control (PVC-only film; no
318 CuDTTCT) and also to the CuDTTCT-casted PVC film (**Figure 5a-e**). The biofilm dispersal effect
319 was enhanced with the presence of 0.4 mM nitrite-Fe²⁺ in the CuDTTCT system, a 45% reduction
320 of the biofilm surface coverage was observed relative to the PVC-only and the CuDTTCT-PVC
321 control (**Figure 5f**). Note the comparable biofilm surface coverage in the CuDTTCT-PVC system
322 as that of the PVC-only system (the '0 mM' and 'control' variation respectively, in Figure 5a),
323 indicating the benign effect of CuDTTCT (and the minimal <1% leached copper ions) on the
324 bacteria attachment/biofilm dispersal, as also observed in our previous work [9]. Further, although
325 (excess of) iron salts has been shown to disrupt biofilms [30,31], such case was not observed in
326 this study, i.e. the presence of Fe²⁺ alone (0.1 to 0.4 mM, in the absence of CuDTTCT) did not
327 cause biofilm dispersal, with similar surface coverage as the control (Supplementary Figure 3).
328 Note that iron limiting condition has been indicated to mediate the formation of biofilms [30-32],
329 which indeed was one of the motives for the use of iron ion as reducing agent in this study. We
330 also found that addition of nitrite into the Fe²⁺-only systems did not cause biofilm dispersal (data
331 not shown), in agreement with earlier studies [29].

332 Recalling the increasing NO generation from the CuDTTCT-nitrite-Fe²⁺ in PBS pH 6 in
333 relevant time frame (200 to 1300 nM maximum NO were generated in 15 to 35 min in the presence
334 of 0.1 to 0.4 mM nitrite-Fe²⁺, **Figure 4**), the increasing biofilm dispersal effect was most likely to
335 result from the catalytic NO generation. The activity of NO to disperse pre-established biofilms,

336 either single- or multi-species, are widely known [7,33–35]. The mechanism for this biofilm-to-
337 free-floating planktonic switch commonly involves NO-mediated alteration of intracellular level
338 of the secondary messenger cyclic di-GMP (c-di-GMP). High c-di-GMP level triggers cell
339 attachment to surfaces and in turn, biofilm formation, while biofilm dispersal and growth in
340 planktonic phase is promoted at low c-di-GMP level. The ‘non-killing’ NO-mediated biofilm
341 dispersal is also observed in the current study with no detection of dead cells, even in system with
342 the highest degree of biofilm dispersal (**Figure 5b-f**). Further, NO has also been reported to reduce
343 aggregation of biomass [36], which is thought to associate to biofilm dispersal mechanism [35].
344 Indeed, we observed less biomass aggregation following treatments of the pre-formed biofilm in
345 the CuDTTCT systems with nitrite-Fe²⁺ (**Figure 5d-f**), compared to the significant biomass
346 aggregation forming in the PVC-only control as well as in the CuDTTCT-PVC control (**Figure**
347 **5a-b**).



348
349 **Figure 5.** (a) Surface coverage analysis of nitrifying bacteria biofilm after addition of nitrite and
350 Fe²⁺ in PBS pH 6. All values shown are normalized to the surface coverage of the control (PVC
351 film). Error bars indicate standard error between replicates (n = 3). **p* ≤ 0.05 compared to the

352 control and 0 mM variation. Confocal laser scanning microscopy images of nitrifying bacteria
353 biofilm (b) grown in the presence of PVC film (control), (c) grown in the presence of CuDTTCT
354 film (0 mM) and (d) treated with 0.1 mM nitrite-Fe²⁺, (e) treated with 0.2 mM nitrite-Fe²⁺, and (f)
355 treated with 0.4 mM nitrite-Fe²⁺. The biofilm growth was in the form of 5 – 50 μm biomass
356 aggregates (analyzed by ImageJ). Green stains denote viable bacteria, whereas red and yellow
357 stains denote non-viable bacteria. Scale bar = 100 μm.
358

359 **4. Conclusion**

360 Herein, the potential of Fe²⁺ ions as an alternative reducing agent was studied for the catalytic
361 generation of NO from nitrite. The work found that the NO generation is influenced by the Fe²⁺
362 availability to facilitate the copper(II)/copper(I) redox cycling of the copper(II) complex
363 (CuDTTCT) catalyst. Amperometric measurement showed that the CuDTTCT-nitrite-Fe²⁺
364 systems generated NO at pH 6 in nitrifying bacteria growth medium but not at pH 8. The
365 phenomenon is thought to result, at least in part, from the lower initial Fe²⁺ availability at the
366 higher pH due to faster Fe²⁺-to-Fe³⁺ autoxidation, that is, the reactions of Fe²⁺ with iron-
367 precipitating moieties such as phosphates and carbonate in the medium. Studying the NO-
368 generating capabilities of the CuDTTCT-nitrite-Fe²⁺ systems in phosphate buffer (PBS), we also
369 observed lower initial Fe²⁺ followed by more rapid depletion of the ions due to autoxidation at pH
370 7 compared to that of at pH 6.5 and 6 and consequently, the higher NO production at the lower
371 pHs. Assessing the performance of the CuDDTCT-nitrite-Fe²⁺ systems at similar pH (with 0.5 mM
372 equimolar nitrite-Fe²⁺), in PBS pH 6 the system generated up to 4000 nM NO and only 280 nM
373 NO in the growth medium pH 6. Such differences appear to stem from the less presence of iron-
374 precipitating moieties in the former system, resulting in slower extent of Fe²⁺-to-Fe³⁺ autoxidation
375 and in turn, higher Fe²⁺ availability. The presence of iron-complexing agent (EDTA) in the growth
376 medium could further limit its Fe²⁺ availability. Ultimately, we observed the biofilm dispersal
377 activity of the CuDTTCT-nitrite-Fe²⁺ catalytic system against pre-formed nitrifying bacteria

378 biofilm in PBS pH 6. While not killing the bacterial cells, the generated NO reduced the extent of
379 cell aggregations. In closing, we have observed the versatility of the copper-based (CuDTTCT)
380 NO-generating catalytic systems, functioning as biofilm dispersants in the presence of the
381 commonly occurring chemical moieties in water, the Fe²⁺ ions and nitrite, suggesting potential
382 applications in the water industries.

383

384 **Acknowledgements**

385 This research was supported under Australian Research Council's Linkage Projects funding
386 scheme (LP110100459). We would like to thank Chemson Pacific Pty. Ltd. for the provision of
387 polyvinyl chloride and Australian Water Quality Centre (SA Water) and Western Australia Water
388 Corporation for the financial support. The authors would also like to thank Dr Jay Hyun-Suk Oh
389 and A/Prof Scott A. Rice (Nanyang Technological University) for the assistance on the NO
390 generation experiment. The authors also acknowledge the support from Mark Wainwright
391 Analytical Centre.

392

393 **Appendix A: Supplementary data**

394 The following is the supplementary data related to this article: catalytic NO generation with excess
395 presence of Fe²⁺, effect of buffer and pH change on nitrifying biofilm surface coverage; effect of
396 ferrous ion addition on nitrifying biofilm surface coverage.

397

398

399

400 **References**

- 401 [1] T. Mattila-Sandholm, G. Wirtanen, Biofilm formation in the industry: A review, Food
402 Rev. Int. 8 (1992) 573–603.
- 403 [2] S.E. Coetser, T.E. Cloete, Biofouling and biocorrosion in industrial water systems., Crit.
404 Rev. Microbiol. 31 (2005) 213–232. <http://www.ncbi.nlm.nih.gov/pubmed/16417202>.
- 405 [3] J.L. Balcazar, J. Subirats, C.M. Borrego, The role of biofilms as environmental reservoirs
406 of antibiotic resistance, Front. Microbiol. 6 (2015) 1–9.
- 407 [4] F. Baquero, J.-L. Martínez, R. Cantón, Antibiotics and antibiotic resistance in water
408 environments, Curr. Opin. Biotechnol. 19 (2008) 260–265.
409 <http://linkinghub.elsevier.com/retrieve/pii/S0958166908000591>.
- 410 [5] A. Bridier, R. Briandet, V. Thomas, F. Dubois-Brissonnet, Resistance of Bacterial
411 Biofilms to Disinfectants: a review., Biofouling. 27 (2011) 1017–1032.
- 412 [6] N. Barraud, D.J. Hassett, S.-H. Hwang, S.A. Rice, S. Kjelleberg, J.S. Webb, Involvement
413 of nitric oxide in biofilm dispersal of *Pseudomonas aeruginosa*., J. Bacteriol. 188 (2006)
414 7344–7353.
- 415 [7] D.P. Arora, S. Hossain, Y. Xu, E.M. Boon, Nitric Oxide Regulation of Bacterial Biofilms,
416 Biochemistry. 54 (2015) 3717–3728.
- 417 [8] A. Friedman, J. Friedman, New biomaterials for the sustained release of nitric oxide: past,
418 present and future., Expert Opin. Drug Deliv. 6 (2009) 1113–22.
- 419 [9] V. Wonoputri, C. Gunawan, S. Liu, N. Barraud, L.H. Yee, M. Lim, R. Amal, Copper
420 Complex in Poly(vinyl chloride) as a Nitric Oxide-Generating Catalyst for the Control of

- 421 Nitrifying Bacterial Biofilms, *ACS Appl. Mater. Interfaces*. 7 (2015) 22148–22156.
- 422 [10] V. Wonoputri, C. Gunawan, S. Liu, N. Barraud, L.H. Yee, M. Lim, R. Amal, Iron
423 Complex Facilitated Copper Redox Cycling for Nitric Oxide Generation as Nontoxic
424 Nitrifying Biofilm Inhibitor, *ACS Appl. Mater. Interfaces*. 8 (2016) 30502–30510.
- 425 [11] C. Opländer, J. Rösner, A. Gombert, A. Brodski, T. Suvorava, V. Grotheer, E.E. van
426 Faassen, K.-D. Kröncke, G. Kojda, J. Windolf, C. V Suschek, Redox-mediated
427 mechanisms and biological responses of copper-catalyzed reduction of the nitrite ion in
428 vitro., *Nitric Oxide*. 35 (2013) 152–164.
- 429 [12] B.K. Oh, M.E. Meyerhoff, Catalytic generation of nitric oxide from nitrite at the interface
430 of polymeric films doped with lipophilic Cu(II)-complex: a potential route to the
431 preparation of thromboresistant coatings, *Biomaterials*. 25 (2004) 283–293.
- 432 [13] A. Pham, A. Rose, T. Waite, Kinetics of Cu (II) reduction by natural organic matter, *J.*
433 *Phys. Chem. A*. 116 (2012) 6590–6599.
- 434 [14] D.L. Sedlak, J. Hoigné, The role of copper and oxalate in the redox cycling of iron in
435 atmospheric waters, *Atmos. Environ. Part A. Gen. Top.* 27 (1993) 2173–2185.
- 436 [15] J.D. Willey, R.F. Whitehead, Oxidation of Fe (II) in Rainwater, *Environ. Sci. Technol.* 39
437 (2005) 2579–2585.
- 438 [16] C.J. Matocha, A.D. Karathanasis, S. Rakshit, K.M. Wagner, Reduction of copper(II) by
439 iron(II)., *J. Environ. Qual.* 34 (2005) 1539–1546.
- 440 [17] A.G. González, N. Pérez-Almeida, J. Magdalena Santana-Casiano, F.J. Millero, M.
441 González-Dávila, Redox interactions of Fe and Cu in seawater, *Mar. Chem.* 179 (2016)

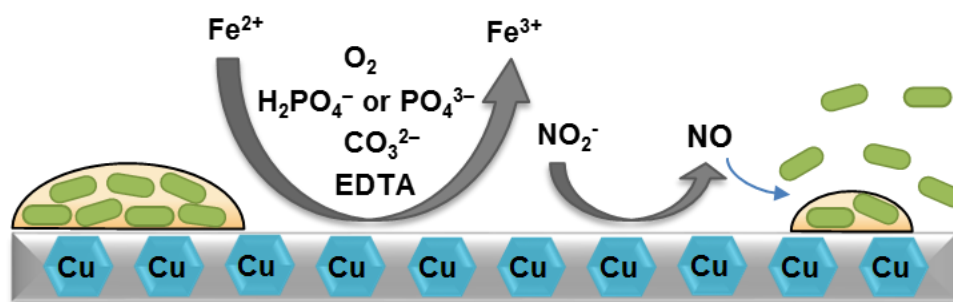
- 442 12–22.
- 443 [18] E.J. O’Loughlin, S.D. Kelly, K.M. Kemner, R. Csencsits, R.E. Cook, Reduction of AgI,
444 AuIII, CuII, and Hg II by FeII/FeIII hydroxysulfate green rust, *Chemosphere*. 53 (2003)
445 437–446.
- 446 [19] S. Mathews, R. Kumar, M. Solioz, Copper reduction and contact killing of bacteria by
447 iron surfaces, *Appl. Environ. Microbiol.* 81 (2015) 6399–6403.
- 448 [20] E. Viollier, P.W. Inglett, K. Hunter, A.N. Roychoudhury, P. Van Cappellen, The ferrozine
449 method revisited: Fe(II)/Fe(III) determination in natural waters, *Appl. Geochemistry*. 15
450 (2000) 785–790.
- 451 [21] B. van der Grift, T. Behrends, L.A. Osté, P.P. Schot, M.J. Wassen, J. Griffioen, Fe
452 hydroxyphosphate precipitation and Fe (II) oxidation kinetics upon aeration of Fe (II)
453 and phosphate-containing synthetic and natural solutions, *Geochim. Cosmochim. Acta*.
454 186 (2016) 71–90.
- 455 [22] K.D. Welch, T.Z. Davis, S.D. Aust, Iron autoxidation and free radical generation: effects
456 of buffers, ligands, and chelators., *Arch. Biochem. Biophys.* 397 (2002) 360–369.
- 457 [23] B. Van Der Grift, J.C. Rozemeijer, J. Griffioen, Y. Van Der Velde, Iron oxidation kinetics
458 and phosphate immobilization along the flow-path from groundwater into surface water,
459 *Hydrol. Earth Syst. Sci.* 18 (2014) 4687–4702.
- 460 [24] S. Baken, C. Moens, B. van der Grift, E. Smolders, Phosphate binding by natural iron-rich
461 colloids in streams, *Water Res.* 98 (2016) 326–333.
- 462 [25] D.W. King, R. Farlow, Role of carbonate speciation on the oxidation rate of Fe (II) by

- 463 H₂O₂, *Mar. Chem.* 70 (2000) 201–209.
- 464 [26] J.O. Lundberg, E. Weitzberg, M.T. Gladwin, The nitrate-nitrite-nitric oxide pathway in
465 physiology and therapeutics., *Nat. Rev. Drug Discov.* 7 (2008) 156–167.
- 466 [27] O. Van Cleemput, L. Baert, Nitrite stability influenced by iron compounds, *Soil Biol.*
467 *Biochem.* 15 (1983) 137–140.
- 468 [28] S. Liu, C. Gunawan, N. Barraud, S.A. Rice, E.J. Harry, R. Amal, Understanding,
469 Monitoring and Controlling Biofilm Growth in Drinking Water Distribution Systems,
470 *Environ. Sci. Technol.* 50 (2016) 8954–8976.
- 471 [29] I. Schmidt, P.J.M. Steenbakkens, H.J.M. op den Camp, K. Schmidt, M.S.M. Jetten,
472 Physiologic and Proteomic Evidence for a Role of Nitric Oxide in Biofilm Formation by
473 *Nitrosomonas europaea* and Other Ammonia Oxidizers, *J. Bacteriol.* 186 (2004) 2781–
474 2788.
- 475 [30] D.J. Musk, D.A. Banko, P.J. Hergenrother, Iron salts perturb biofilm formation and
476 disrupt existing biofilms of *Pseudomonas aeruginosa*, *Chem. Biol.* 12 (2005) 789–796.
- 477 [31] L. Yang, K.B. Barken, M.E. Skindersoe, A.B. Christensen, M. Givskov, T. Tolker-
478 Nielsen, Effects of iron on DNA release and biofilm development by *Pseudomonas*
479 *aeruginosa*, *Microbiology.* 153 (2007) 1318–1328.
- 480 [32] M. Johnson, A. Cockayne, J.A. Morrissey, Iron-Regulated Biofilm Formation in
481 *Staphylococcus aureus* Newman Requires *ica* and the Secreted Protein Emp Iron-
482 Regulated Biofilm Formation in *Staphylococcus aureus* Newman Requires *ica* and the
483 Secreted Protein Emp, *Infect. Immun.* 76 (2008) 1756–1765.

- 484 [33] D. McDougald, S.A. Rice, N. Barraud, P.D. Steinberg, S. Kjelleberg, Should we stay or
485 should we go: mechanisms and ecological consequences for biofilm dispersal, *Nat. Rev.*
486 *Microbiol.* 10 (2011) 39–50.
- 487 [34] M. Craven, S.H. Kasper, M. Canfield, R. Diaz-Morales, J. Hrabie, N.C. Cady, A.
488 Strickland, Nitric Oxide-Releasing Polyacrylonitrile Disperses Biofilms Formed by
489 Wound-Relevant Pathogenic Bacteria, *J. Appl. Microbiol.* 120 (2016) 1085–1099.
- 490 [35] N. Barraud, M. V Storey, Z.P. Moore, J.S. Webb, S.A. Rice, S. Kjelleberg, Nitric oxide-
491 mediated dispersal in single- and multi-species biofilms of clinically and industrially
492 relevant microorganisms, *Microb. Biotechnol.* 2 (2009) 370–378.
- 493 [36] S. Schlag, C. Nerz, T.A. Birkenstock, F. Altenberend, F. Götz, Inhibition of
494 staphylococcal biofilm formation by nitrite, *J. Bacteriol.* 189 (2007) 7911–7919.

495

496 **Graphical Abstract**



497